Published in final edited form as:
Circulation. 2009 July 28; 120(4): 334–342. doi:10.1161/CIRCULATIONAHA.108.846782.

Active Adaptation of the Tethered Mitral Valve: Insights into a Compensatory Mechanism for Functional Mitral Regurgitation

Jacob P. Dal-Bianco, MD, **Elena Aikawa, MD, PhD**[*], **Joyce Bischoff, PhD**[*], **J. Luis Guerrero, BS**, **Mark D. Handschumacher, BS**, **Suzanne Sullivan, BS**, **Benjamin Johnson, BA**, **James S Titus, BS**, **Yoshiko Iwamoto, BS**, **Jill Wylie-Sears, MS**, **Robert A. Levine, MD**[**], and **Alain Carpentier, MD, PhD**[**]

1) Cardiac Ultrasound Laboratory (JPD, MDH, RAL) and Surgical Cardiovascular Laboratory (JLG, SS, BJ, JT), Massachusetts General Hospital, Harvard Medical School, Boston, MA; 2) Vascular Biology Program (JW-S, JB) and Department of Surgery (JB), Children's Hospital Boston and Harvard Medical School, Boston, MA; 3) Center for Molecular Imaging Research (EA, YI), Massachusetts General Hospital and Harvard Medical School, Charlestown, MA; 4) Department of Cardiovascular Surgery (AC), Pompidou Hospital, and INSERM Unit 633, Paris, France; 5) Leducq Transatlantic MITRAL Network (JPD, EA, JB, RAL, AC)

Abstract

Background—In patients with left ventricular infarction or dilatation, leaflet tethering by displaced papillary muscles (PMs) frequently induces mitral regurgitation (MR), which doubles mortality. Little is known about mitral valve (MV) biological potential to compensate for ventricular remodeling. We tested the hypothesis that MV leaflet surface area increases over time with mechanical stretch created by PM displacement through cell activation, not passive stretching.

Methods and Results—Under cardiopulmonary bypass, the PM tips in 6 adult sheep were retracted apically short of producing MR to replicate tethering without confounding MI or turbulence. Diastolic leaflet area was quantified by 3D-echo over 61±6 days, compared with 6 unstretched sheep MVs. Total diastolic leaflet area increased by 2.4±1.3cm^2 (17±10%) from 14.3±1.9cm^2 to 16.7 ±1.9cm^2 (p=0.006) with stretch, without change in unstretched valves despite sham open-heart surgery. Stretched MVs were 2.8 times thicker than normal (1.18±0.14 vs 0.42±0.14mm, p<0.0001) at sacrifice, with increased spongiosa layer. Endothelial cells (CD31+) co-expressing α-smooth muscle actin (α-SMA) were significantly more common by fluorescent cell sorting in tethered versus normal leaflets (41±19% vs 9±5%, p=0.02), indicating endothelial-mesenchymal transdifferentiation

Correspondence: Robert A. Levine, MD, Massachusetts General Hospital, Cardiac Ultrasound Laboratory, 55 Fruit Street, Yawkey 5068, Boston, MA 02114, rlevine@partners.org.

[*]These authors contributed equally to the publication.

[**]Senior authorship is acknowledged for Drs. Carpentier and Levine to reflect this cross-disciplinary collaboration and their unique contributions

Disclosures: None.

Clinical Perspective: Mitral regurgitation is a frequent complication of myocardial infarction that doubles heart failure and mortality and is caused by stretch of the mitral leaflets by damaged and bulging heart walls preventing effective valve closure. Compensatory valve growth could reduce mitral regurgitation. A recent patient study showed significantly enlarged leaflets in patients with left ventricular dysfunction compared to normals; whether the valve actively grows over time or is just passively stretched is unknown. The individual effects of ischemia, regurgitant jet flow and leaflet stretch on potential valve adaptation, all present in ischemic MR, are also unknown. This study combined a new model producing isolated and controlled leaflet stretch with a noninvasive technique for quantifying valve area changes over time, in an interdisciplinary collaboration with basic scientists. Two months of leaflet stretch by apical papillary muscle retraction reactivated embryonic development pathways, resulting in valvular and chordal growth shown by cellular activation, transformation of endothelial to interstitial cells, and new matrix deposition. Leaflet surface area and both leaflet and chordal thickness increased substantially relative to baseline and unstretched controls. The mitral valve therefore actively adapts in this setting. Understanding the mechanisms of such active adaptation can potentially provide therapeutic opportunities to augment MV area and reduce ischemic MR.

(EMT); α-SMA-positive cells appeared in the atrial endothelium, penetrating into the interstitium, with increased collagen deposition. Thickened chordae showed endothelial and subendothelial α-SMA. EMT capacity was also demonstrated in cultured endothelial cells.

Conclusion—Mechanical stresses imposed by PM tethering increase MV leaflet area and thickness, with cellular changes suggesting reactivated embryonic development pathways. Understanding such actively adaptive mechanisms can potentially provide therapeutic opportunities to augment MV area and reduce ischemic MR.

Keywords

echocardiography; valves; mitral valve

In population studies, valvular heart disease is common, with mitral regurgitation (MR) most prevalent [1]. Although degeneration is the leading cause of MR surgical repair [2], coronary artery disease with myocardial infarction (MI) and left ventricular (LV) dysfunction frequently causes functional MR due to global LV remodeling and sphericity [3-5] or localized inferoposterior wall remodeling [6-11]; both cause apical, posterior and outward displacement of the papillary muscles (PMs) [6-12] and mitral valve (MV) leaflet tethering [13] that prevents effective closure (Figure 1A&B) [12, 14].

Patients who develop MR post-MI or with congestive heart failure, even after surgical or catheter revascularization, have doubled mortality and increased cardiac complications [15-17]. It is reasonable to suppose that an increase in MV leaflet surface area might compensate for ventricular remodeling, and that the stressed MV, like other biological structures, might adapt by enlargement. However, little is known about MV tissue biology and potential for adaptation. Decreased leaflet distensibility has been reported in severe heart failure patients [18, 19], but not correlated with total leaflet area. MV leaflets acutely and reversibly elongate up to 15% under physiologic tension [20, 21], and recent work in 80 patients has shown that MV leaflet surface area measured by three-dimensional echocardiography (3D echo) is greater by an average of 35% in patients with chronically tethered leaflets compared with normal controls [22]. Leaflet area, however, failed to increase in proportion to the geometric demands (three-dimensional tenting) imposed by PM displacement in patients with ischemic MR, in contrast to those with LV remodeling and no MR. Larger leaflets may therefore partially compensate for tethering. Current data, however, provide no proof that leaflet area actually increases over time within a given patient. It is also unknown whether the leaflets enlarge because of passive stretching or active remodeling and growth, with increased cell content and matrix production. Leaflet elongation has recently been reported in a heart failure model in systole, when passive stretch may be superimposed on actual tissue growth [23]. The ability to study leaflet adaptation to stretch in standard ischemic MR models may also be confounded by several factors, including myocardial ischemia and infarction, which may cause fibrosis by secretion of growth signals such as transforming growth factor-beta superfamily members (TGF-β) [24] and periostin [25]; turbulent MR flow itself appears to induce localized secondary lesions [26]; isolated MR increases matrix turnover [27]; and cardiac medications affect vascular response to growth factors [28].

In order to observe leaflet adaptation to tethering over time, we assembled a team to study MV cell biology and molecular pathways and designed a large-animal model that allows independent and controlled leaflet tethering without confounding ischemia or turbulent MR flow. 3D echo allows leaflet area quantification at different times in the same heart. Using these resources, we tested the hypothesis that MV surface area increases over time with mechanical stretch, and as a consequence of cell activation and matrix production as opposed to passive stretching.

Methods

Animal Care

Twelve adult Dorsett hybrid sheep (weight>45kg) were loaded for 3 days with Amiodarone (200mg orally/day), then anesthetized (Thiopentothal sodium 12.5ml/kg IV), intubated and ventilated at 15 ml/kg with 2% Isoflurane-oxygen adjusted by blood-oxygen and CO_2 monitoring. Animals prophylactically received Glycopyrrolate (0.4mg intravenously), Cephazolin (0.5gm intravenously) and Amiodarone (150mg intravenous drip) during surgery, and intravenous lactated ringer solution as needed.

Experimental Model

Based on Prof. Alain Carpentier's suggestion, PM retraction and leaflet tethering were achieved using a technique developed by the authors (JLG, JDB) to overcome the challenge of tethering leaflets in a controlled fashion without producing MR or leaflet tissue disruption. After sterile left thoracotomy and pericardial cradle construction, under cardiopulmonary bypass, suture loops were inserted into the exposed PM tips (both medial PM heads), buttressed by Teflon felt pledgets and exteriorized to the epicardium overlying the apical insertion of the PMs. These sutures then paralleled the PM axis, and retracting them pulled the PM tip and leaflets toward the apex (Figure 1C&D).

After the heart was re-started, suture length was adjusted just short of producing MR under echo guidance, and the sutures were fixed to an anchoring Dacron patch attached to the apical epicardium to spread out local myocardial pressure over a larger area and avoid underlying ischemia. MV leaflets were tethered in 6 sheep cared for over 61±6 days, followed by left thoracotomy for high-quality imaging and 3D reconstruction of MV surface area after the 2 months of mechanical tethering. After sacrifice the heart was sterilely harvested.

Sheep with tethered MV leaflets (n=6) were compared with a group of 6 sheep with normal, unstretched MVs. Three of these sheep had bypass surgery and no leaflet tethering and were followed over the same 2-month time.

These studies conform to NIH guidelines for animal care and have Institutional Animal Care Committee approval.

Echocardiography

Doppler echo data were collected epicardially using a high-frequency (3.5-5 MHz) TTE probe. 2D and 3D echo probes (S5, X3) interfaced with a Philips iE33 scanner (Andover, MA). 3D volumetric data sets were ECG-gated from 4-7 consecutive heartbeats. Full data sets were acquired in standardized planes at baseline and before sacrificing. MR presence or absence and grade based on long-axis-view vena contracta [29] and successful MV leaflet tethering were immediately assessed. Data were digitally stored for offline analysis using Xcelera and QLAB 5.1 (Philips, Andover, MA), and the custom software Omni4D (MD Handschumacher).

Total MV leaflet area can be measured precisely only in diastole, since in systole the area of each leaflet involved in coaptation cannot be optimally resolved. Measuring diastolic leaflet area also evaluates adaptation when LV pressure and leaflet tension are minimal without passive systolic stretch [13]. Therefore, total leaflet area in full diastolic opening was analyzed using Omni4D, as validated against excised MV specimens in 15 sheep [22] with excellent correlation and agreement (R^2=0.86, SEE=1.24, mean difference=0.51±1.15, p=0.71). All offline echo data were measured in a blinded fashion by a single observer.

Mitral valve tissue harvesting

Sheep hearts were harvested, the left atrium opened and LV wall dissected starting at the anterolateral commissure in a sterile manner under irrigation of pre-cooled phosphate buffered saline (PBS). Anterior and posterior leaflets with chordae and papillary muscles were dissected and divided for histopathology (frozen in OCT compound and stored at -80° C) and cell isolation and flow-cytometry (transported fresh in cooled physiologic collecting medium).

Histology

Overall MV morphology was analyzed using hematoxylin and eosin stain. MV and chordae collagen architecture was detected by Masson's trichrome staining. Leaflet thickness was measured by microscopy in ten thickest areas across the midportion of the anterior and posterior leaflets, and similarly explored for the leaflet bases and tips. Chordal length and thickness (anterior and posterior strut chordae) were measured on calibrated gross pathology photographs from PM tip to furthest leaflet insertion (Adobe, San Jose, California); thickness of ten randomly selected chords was measured by microscopy. Endothelial cells (EC) were identified using anti-CD31 antibody (Santa Cruz Biotechnology). The activated valvular interstitial cell (VIC) phenotype was determined by immunohistochemistry for myofibroblast markers (anti-α-smooth muscle actin [anti-α-SMA]; clone 1A4; Sigma)) [30-33]. In addition, to show the clinical relevance of our model, we obtained excised MV leaflets from patients with ischemic MR (n=4).

MV cell analysis

The aim was to determine whether valve ECs expressing CD31 are altered in tethered leaflets and also express the interstitial cell marker α-SMA. This would indicate that the valve endothelium is an adaptive reservoir for adding interstitial cells through endothelial-mesenchymal transdifferentiation (EMT).

Valve tissue was minced into 1mm × 1mm pieces and digested with Cell Dissociation Buffer (Invitrogen) for 4-minutes at 37 C at a specific tissue/volume ratio to obtain a single-cell suspension of endothelial and interstitial cells and quantify valvular cells transitioning to a mesenchymal phenotype by flow cytometry. ECs were detected and quantified using murine anti-sheep CD31 antibody conjugated to fluorescein isothyocyanate (FITC, ABD Serotec); activated cells were detected using a murine anti-human α-SMA (clone1A4) conjugated to phycoerythrin (R&D Systems). Anterior and posterior leaflets were analyzed separately.

Direct demonstration of capacity for EMT

Aortic and pulmonary valve endothelial cells have been induced to undergo EMT *in vitro* [30, 33, 34], but that has not been shown before for MV ECs. Therefore, as an ancillary study to test directly whether MV ECs are competent to undergo EMT, we isolated clonal MV EC populations, treated them with TGF-β isoforms 1, 2 and 3 (1 ng/ml for 5 days), and evaluated onset of α-SMA expression, widely regarded as a marker for EMT [35], by immunostaining and Western blot of cell lysates.

Sample size and power

We hypothesized that chronic tethering will result in a 25% increase in leaflet area, consistent with clinical and pilot data. To demonstrate such changes with 5% alpha error and 80% power, a minimum of 5 animals/group were required.

Statistics

Data are summarized as mean±SD for continuous variables. Paired Student's t-test compared baseline and sacrifice results within the same animal. Student t-test compared continuous variables between groups. Statistical significance was set at $p<0.05$.

Statement of Responsibility

The authors had full access to the data and take responsibility for its integrity. All authors have read and agree to the manuscript as written.

Results

The experimental model uniformly produced PM retraction and mildly tented mitral leaflets (Figure 1D) consistent with tethering, confirmed by increased tenting volume between annulus and leaflets (Table 1). No animal had more than mild MR at baseline or follow-up studies, with no significant change in MR vena contracta (VC) from baseline (Table 1).

Leaflet anatomy

Total diastolic MV leaflet area consistently increased by an average of 2.4±1.3cm^2 (17±10%) from 14.3±1.9cm^2 to 16.7±1.9cm^2 ($p=0.006$) with maintained stretch, without significant change in unstretched valves despite sham open-heart surgery (14.5±1.2cm^2 to 14.7±2cm^2; $p=0.9$). Leaflet area did not increase more (8%) in the one sheep that developed mild MR (VC=0.38cm). Leaflet length also increased significantly over time in the stretched MVs (Table 1). Gross pathology at sacrifice showed increased leaflet size and opacity, consistent with increased thickness (Figure 2). By histology, stretched MVs were 2.8 times thicker than normal at their midportions (1.18±0.14 vs 0.42±0.14mm, $p<0.0001$) with increased spongiosa layer (Figure 3). Leaflet thickness also increased >60% in both the leaflet body and distal tip in sham versus stretched MVs (Table 2). Diastolic annular area increased by an average of 15%, without change in the ratio of leaflet/annular area (1.73±0.17 versus 1.74±0.15, $p=0.9$) – a ratio that is likewise comparable in patients with tethered versus normal leaflets [22].

Chordal anatomy

Anterior and posterior chordae were significantly thicker (Figure 2&4, left) and longer in stretched versus unstretched MVs, both for photographic measurements of the thicker strut chordae and averaged microscopic chordal thickness (Table 2).

EMT in MV leaflets

By flow cytometry, endothelial cells (CD31+) co-expressing α-SMA were significantly more common in tethered anterior and posterior leaflets versus untethered leaflets, comprising 41 ±19% vs 9±5% of all ECs, $p=0.02$ (Figure 5A&B).

Molecular histopathology

Unstretched MV leaflets and chordae showed CD31+ cells along the endothelial layer without α-SMA staining (Figure 6, left). In contrast, stretched leaflets consistently showed both CD31 and α-SMA staining in the endothelial layer, indicating activation/EMT, almost exclusively along the atrial border; individual α-SMA+ cells also appeared to penetrate the valve interstitium (Figure 6, right). Figure 7 shows another stretched valve with α-SMA+ cells penetrating the interstitium; Masson's trichrome staining indicates increased collagen deposition around those cells. Stretched chordae also showed endothelial-cell positive α-SMA staining and accumulation of α-SMA-positive myofibroblasts below endothelium (Figure 4, right) with decreased collagen alignment and density.

Cell activation and EMT in human ischemic MR

Immunohistochemistry of MV leaflets from all four patients with ischemic MR showed α-SMA expression in the endothelium and in VICs throughout the leaflets (Figure 8), suggesting that human diseased valves undergo EMT and VIC activation similar to those detected in the sheep model.

Capacity of MV ECs for EMT: direct demonstration

Figures 5C&D show that beginning with a MV EC clone with documented endothelial phenotype (CD31+/α-SMA-), TGF-β 1,2 and 3 all induced α-SMA expression. Therefore, similar to post-natal aortic and pulmonary valve ECs [30, 33, 34], mitral valve ECs can also be induced to undergo EMT.

Discussion

This experimental study goes beyond prior clinical observations and proves that tethered MV leaflets increase in area within the same heart over time by activation of cells and thickening of the interstitial matrix, with an altered cell biology indicating endothelial-mesenchymal transdifferentiation (EMT), characterized by dual labeling for endothelial and interstitial cell markers in both leaflets and chordae.

Developmental perspective

During embryonic cardiac valve development, factors such as TGF-β, bone morphogenetic proteins, epidermal growth factor and vascular endothelial growth factor, along with Notch, signal endothelial cells overlying myocytes to lose cell-cell contacts, migrate into the cardiac jelly (primordial valve interstitium), reduce expression of endothelial markers and gain mesenchymal markers such as α-SMA (Figure 6, lower panel) [36-39]. This endothelial-mesenchymal cell transdifferentiation forms the endocardial cushions, the primordia of the cardiac valves and septa [40]. Post-EMT cushion valvular maturation seems to be regulated by the same signals and fibroblast growth factor [41]. Subsequent leaflet delamination from the ventricular wall relates in part to periostin, a protein secreted by fibroblasts.

After embryonic development and throughout adult life, human valves maintain cell plasticity (quiescent fibroblasts > activated myofibroblasts detected by α-SMA) and dynamic structure (nascent extracellular matrix) to respond to hemodynamic changes. In this study, the high prevalence of α-SMA-positive cells and their interstitial penetration in stretched valves suggests reactivated embryonic valve developmental pathways / EMT and supports the concept of an actively adapting MV [42]. This process appears to begin on the atrial layer (Figures 6, 7, 8); a possible explanation is that this layer, with its higher radius of curvature, bears high mechanical stresses by Laplace's law [43]; alternatively, the atrial and ventricular endothelia may have biological differences [44].

Clinical observations

This study is entirely based on the animal model. However, to begin exploring whether the findings have a clinical counterpart, particularly in more chronic tethering, we examined human MVs affected by ischemic MR (n=4), all of which had similar α-SMA-positive cell activation and distribution as in the animal model (Figure 8), apparently as an ongoing process despite advanced age (71±2.6y) and disease chronicity.

Mechanism and therapeutic implications

Increased leaflet length and interstitial thickness have been observed in a Marfan syndrome mouse model [45], correlated with TGF-β activation. Mechanical stresses caused by PM tethering

may upregulate TGF-β [46], which, as we have shown, induces EMT in MV ECs; increased TGF-β could similarly explain increased leaflet length and interstitial thickness in our model. Ischemic myocardium may also stimulate MV leaflet growth and collagen production [47] by secreting TGF-β, which is elevated in both infarcted and remote noninfarcted myocardium [48]. The turbulent MR jet may further signal the MV leaflets to change, as suggested by Carpentier based on localized thickening of otherwise thin MVs in regions of chordal rupture [26]. The ischemic and volume-overload lesions [27], however, may have other local and paracrine effects on valve growth that may help explain the frequent insufficiency of leaflet adaptation to prevent MR [22].

Understanding the mechanisms of MV adaptation has potential therapeutic implications, with the long-range goal of augmenting MV area to reduce ischemic MR. There is growing recognition that the TGF-β pathways influencing valve growth are susceptible to pharmacologic modification. For example, using an angiotensin receptor blocker as a TGF-β antagonist has been shown to limit tissue growth in a Marfan mouse model [28], and is now undergoing clinical trials. Converse approaches might augment the adaptive process in remodeled LVs while also preserving physiologic leaflet biomechanics [49]. Surgical strategies may also incorporate leaflet augmentation to improve repair efficacy.

Models, limitations, and future directions

These results are consistent with those of Timek, Miller, et al., in a sheep pacing-induced cardiomyopathy model using radioopaque markers along the leaflet midline [23]. Systolic leaflet length increased over 15 days, although the tethering distance from the PMs to the annulus did not appear to increase, in contrast to the inferior MI situation [6, 7].

Diastolic leaflet area was measured in the present study to separate out the effects of valve adaptation: systolic area might be different in hearts with stretched versus unstretched valves because of both valve growth and passive systolic stretch. In addition, in systole, the juxtaposed coapted leaflet areas cannot be optimally resolved [13].

Although isolated mechanical stretch is only one element of the ischemic MR substrate, the leaflet stretch model allows isolation of mechanical, ischemic, and MR flow components to test their influence on valve growth alone and in combination. The purpose of this study, however, was specifically to focus on the influence of leaflet stretch. This model also provides a platform for subsequently studying controlled changes in other factors.

The model allows standardization of the PM stretch to produce leaflet tenting but with no more than mild MR (Figure 1D). Direct staining and quantitative analysis of TGF-β and related signaling pathways are being done in follow-up studies. Adequacy of chordal changes and the nature and role of annular enlargement, not areas of initial focus, also warrant further investigation, including precise delineation of chordal length and insertion. The role of intrinsic and hematopoietic-derived progenitor cells in leaflet adaptation [34, 50] will also require additional analytic approaches.

Conclusion

Mechanical stresses imposed by PM tethering increase MV leaflet area and matrix thickness, with cellular changes suggestive of reactivated embryonic valve development pathways. These findings support the concept of an actively adapting MV; understanding adaptive mechanisms can potentially provide therapeutic opportunities to augment MV area and reduce ischemic MR.

Acknowledgments

This work was presented at the 81st Scientific Sessions of the American Heart Association, New Orleans, Louisiana, November 2008 in the finals of the Samuel A. Levine Young Clinical Investigator Awards competition.

We thank Shirley Sims for her expert editorial assistance.

Funding Sources: This work was supported in part by grant 07CVD04 from the Fondation Leducq, Paris, France, for the Transatlantic MITRAL Network of Excellence, grants K24 HL67434 and R01 HL38176 of the National Institutes of Health (Bethesda, MD) and an American Society of Echocardiography Career Development Award (J.P.D.).

References

1. Nkomo VT, Gardin JM, Skelton TN, Gottdiener JS, Scott CG, Enriquez-Sarano M. Burden of valvular heart diseases: a population-based study. Lancet 2006;368:1005–1011. [PubMed: 16980116]
2. Waller BF, Morrow AG, Maron BJ, Del Negro AA, Kent KM, McGrath FJ, Wallace RB, McIntosh CL, Roberts WC. Etiology of clinically isolated, severe, chronic, pure mitral regurgitation: analysis of 97 patients over 30 years of age having mitral valve replacement. Am Heart J 1982;104:276–288. [PubMed: 7102512]
3. Kaul S, Spotnitz WD, Glasheen WP, Touchstone DA. Mechanism of ischemic mitral regurgitation. An experimental evaluation. Circulation 1991;84:2167–2180. [PubMed: 1934385]
4. Otsuji Y, Handschumacher MD, Schwammenthal E, Jiang L, Song JK, Guerrero JL, Vlahakes GJ, Levine RA. Insights from three-dimensional echocardiography into the mechanism of functional mitral regurgitation: direct in vivo demonstration of altered leaflet tethering geometry. Circulation 1997;96:1999–2008. [PubMed: 9323092]
5. Sabbah HN, Kono T, Stein PD, Mancini GB, Goldstein S. Left ventricular shape changes during the course of evolving heart failure. Am J Physiol 1992;263:H266–270. [PubMed: 1636764]
6. Yiu SF, Enriquez-Sarano M, Tribouilloy C, Seward JB, Tajik AJ. Determinants of the degree of functional mitral regurgitation in patients with systolic left ventricular dysfunction: A quantitative clinical study. Circulation 2000;102:1400–1406. [PubMed: 10993859]
7. Otsuji Y, Handschumacher MD, Liel-Cohen N, Tanabe H, Jiang L, Schwammenthal E, Guerrero JL, Nicholls LA, Vlahakes GJ, Levine RA. Mechanism of ischemic mitral regurgitation with segmental left ventricular dysfunction: three-dimensional echocardiographic studies in models of acute and chronic progressive regurgitation. J Am Coll Cardiol 2001;37:641–648. [PubMed: 11216991]
8. He S, Fontaine AA, Schwammenthal E, Yoganathan AP, Levine RA. Integrated mechanism for functional mitral regurgitation: leaflet restriction versus coapting force: in vitro studies. Circulation 1997;96:1826–1834. [PubMed: 9323068]
9. Gorman RC, McCaughan JS, Ratcliffe MB, Gupta KB, Streicher JT, Ferrari VA, St John-Sutton MG, Bogen DK, Edmunds LH Jr. Pathogenesis of acute ischemic mitral regurgitation in three dimensions. J Thorac Cardiovasc Surg 1995;109:684–693. [PubMed: 7715215]
10. Llaneras MR, Nance ML, Streicher JT, Lima JA, Savino JS, Bogen DK, Deac RF, Ratcliffe MB, Edmunds LH Jr. Large animal model of ischemic mitral regurgitation. Ann Thorac Surg 1994;57:432–439. [PubMed: 8311608]
11. Komeda M, Glasson JR, Bolger AF, Daughters GT 2nd, MacIsaac A, Oesterle SN, Ingels NB Jr, Miller DC. Geometric determinants of ischemic mitral regurgitation. Circulation 1997;96:II-128–133.
12. Godley RW, Wann LS, Rogers EW, Feigenbaum H, Weyman AE. Incomplete mitral leaflet closure in patients with papillary muscle dysfunction. Circulation 1981;63:565–571. [PubMed: 7460242]
13. Nielsen SL, Nygaard H, Fontaine AA, Hasenkam JM, He S, Andersen NT, Yoganathan AP. Chordal force distribution determines systolic mitral leaflet configuration and severity of functional mitral regurgitation. J Am Coll Cardiol 1999;33:843–853. [PubMed: 10080490]
14. Levine RA, Schwammenthal E. Ischemic mitral regurgitation on the threshold of a solution: from paradoxes to unifying concepts. Circulation 2005;112:745–758. [PubMed: 16061756]

15. Grigioni F, Enriquez-Sarano M, Zehr KJ, Bailey KR, Tajik AJ. Ischemic mitral regurgitation: long-term outcome and prognostic implications with quantitative Doppler assessment. Circulation 2001;103:1759–1764. [PubMed: 11282907]
16. Lamas GA, Mitchell GF, Flaker GC, Smith SC Jr, Gersh BJ, Basta L, Moye L, Braunwald E, Pfeffer MA. Clinical significance of mitral regurgitation after acute myocardial infarction. Survival and Ventricular Enlargement Investigators. Circulation 1997;96:827–833. [PubMed: 9264489]
17. Picard MH, Davidoff R, Sleeper LA, Mendes LA, Thompson CR, Dzavik V, Steingart R, Gin K, White HD, Hochman JS. Echocardiographic predictors of survival and response to early revascularization in cardiogenic shock. Circulation 2003;107:279–284. [PubMed: 12538428]
18. Grande-Allen KJ, Barber JE, Klatka KM, Houghtaling PL, Vesely I, Moravec CS, McCarthy PM. Mitral valve stiffening in end-stage heart failure: evidence of an organic contribution to functional mitral regurgitation. J Thorac Cardiovasc Surg 2005;130:783–790. [PubMed: 16153929]
19. Grande-Allen KJ, Borowski AG, Troughton RW, Houghtaling PL, Dipaola NR, Moravec CS, Vesely I, Griffin BP. Apparently normal mitral valves in patients with heart failure demonstrate biochemical and structural derangements: an extracellular matrix and echocardiographic study. J Am Coll Cardiol 2005;45:54–61. [PubMed: 15629373]
20. Kunzelman KS, Cochran RP. Stress/strain characteristics of porcine mitral valve tissue: parallel versus perpendicular collagen orientation. J Card Surg 1992;7:71–78. [PubMed: 1554980]
21. May-Newman K, Yin FC. Biaxial mechanical behavior of excised porcine mitral valve leaflets. Am J Physiol 1995;269:H1319–1327. [PubMed: 7485564]
22. Chaput M, Handschumacher MD, Tournoux F, Hua L, Guerrero JL, Vlahakes GJ, Levine RA. Mitral leaflet adaptation to ventricular remodeling: occurrence and adequacy in patients with functional mitral regurgitation. Circulation 2008;118:845–852. [PubMed: 18678770]
23. Timek TA, Lai DT, Dagum P, Liang D, Daughters GT, Ingels NB Jr, Miller DC. Mitral leaflet remodeling in dilated cardiomyopathy. Circulation 2006;114:I518–523. [PubMed: 16820630]
24. Seo D, Hare JM. The transforming growth factor-beta/Smad3 pathway: coming of age as a key participant in cardiac remodeling. Circulation 2007;116:2096–2098. [PubMed: 17984387]
25. Shimazaki M, Nakamura K, Kii I, Kashima T, Amizuka N, Li M, Saito M, Fukuda K, Nishiyama T, Kitajima S, Saga Y, Fukayama M, Sata M, Kudo A. Periostin is essential for cardiac healing after acute myocardial infarction. J Exp Med 2008;205:295–303. [PubMed: 18208976]
26. Fornes P, Heudes D, Fuzellier JF, Tixier D, Bruneval P, Carpentier A. Correlation between clinical and histologic patterns of degenerative mitral valve insufficiency: a histomorphometric study of 130 excised segments. Cardiovasc Pathol 1999;8:81–92. [PubMed: 10724505]
27. Stephens EH, Nguyen TC, Itoh A, Miller DC, Grande-Allen KJ. Abstract 1158: Mitral Leaflet Remodeling: Response to Isolated Mitral Regurgitation. Circulation 2007;116:II_234.
28. Habashi JP, Judge DP, Holm TM, Cohn RD, Loeys BL, Cooper TK, Myers L, Klein EC, Liu G, Calvi C, Podowski M, Neptune ER, Halushka MK, Bedja D, Gabrielson K, Rifkin DB, Carta L, Ramirez F, Huso DL, Dietz HC. Losartan, an AT1 antagonist, prevents aortic aneurysm in a mouse model of Marfan syndrome. Science 2006;312:117–121. [PubMed: 16601194]
29. Mele D, Vandervoort P, Palacios I, Rivera JM, Dinsmore RE, Schwammenthal E, Marshall JE, Weyman AE, Levine RA. Proximal jet size by Doppler color flow mapping predicts severity of mitral regurgitation. Clinical studies. Circulation 1995;91:746–754. [PubMed: 7828303]
30. Aikawa E, Whittaker P, Farber M, Mendelson K, Padera RF, Aikawa M, Schoen FJ. Human semilunar cardiac valve remodeling by activated cells from fetus to adult: implications for postnatal adaptation, pathology, and tissue engineering. Circulation 2006;113:1344–1352. [PubMed: 16534030]
31. Rabkin E, Aikawa M, Stone JR, Fukumoto Y, Libby P, Schoen FJ. Activated interstitial myofibroblasts express catabolic enzymes and mediate matrix remodeling in myxomatous heart valves. Circulation 2001;104:2525–2532. [PubMed: 11714645]
32. Rabkin E, Hoerstrup SP, Aikawa M, Mayer JE Jr, Schoen FJ. Evolution of cell phenotype and extracellular matrix in tissue-engineered heart valves during in-vitro maturation and in-vivo remodeling. J Heart Valve Dis 2002;11:308–314. [PubMed: 12056720]discussion 314
33. Rabkin-Aikawa E, Aikawa M, Farber M, Kratz JR, Garcia-Cardena G, Kouchoukos NT, Mitchell MB, Jonas RA, Schoen FJ. Clinical pulmonary autograft valves: pathologic evidence of adaptive remodeling in the aortic site. J Thorac Cardiovasc Surg 2004;128:552–561. [PubMed: 15457156]

34. Paranya G, Vineberg S, Dvorin E, Kaushal S, Roth SJ, Rabkin E, Schoen FJ, Bischoff J. Aortic valve endothelial cells undergo transforming growth factor-beta-mediated and non-transforming growth factor-beta-mediated transdifferentiation in vitro. Am J Pathol 2001;159:1335–1343. [PubMed: 11583961]
35. Person AD, Klewer SE, Runyan RB. Cell biology of cardiac cushion development. Int Rev Cytol 2005;243:287–335. [PubMed: 15797462]
36. Armstrong EJ, Bischoff J. Heart valve development: endothelial cell signaling and differentiation. Circ Res 2004;95:459–470. [PubMed: 15345668]
37. Yang JH, Wylie-Sears J, Bischoff J. Opposing actions of Notch1 and VEGF in post-natal cardiac valve endothelial cells. Biochem Biophys Res Commun 2008;374:512–516. [PubMed: 18647596]
38. Bernanke DH, Markwald RR. Migratory behavior of cardiac cushion tissue cells in a collagen-lattice culture system. Dev Biol 1982;91:235–245. [PubMed: 7095266]
39. Nakajima Y, Mironov V, Yamagishi T, Nakamura H, Markwald RR. Expression of smooth muscle alpha-actin in mesenchymal cells during formation of avian endocardial cushion tissue: a role for transforming growth factor beta3. Dev Dyn 1997;209:296–309. [PubMed: 9215644]
40. Markwald RR, Fitzharris TP, Manasek FJ. Structural development of endocardial cushions. Am J Anat 1977;148:85–119. [PubMed: 842477]
41. Butcher JT, Markwald RR. Valvulogenesis: the moving target. Philos Trans R Soc Lond B Biol Sci 2007;362:1489–1503. [PubMed: 17569640]
42. Schoen FJ. Evolving concepts of cardiac valve dynamics: the continuum of development, functional structure, pathobiology, and tissue engineering. Circulation 2008;118:1864–1880. [PubMed: 18955677]
43. Arts T, Meerbaum S, Reneman R, Corday E. Stresses in the closed mitral valve: a model study. J Biomech 1983;16:539–547. [PubMed: 6619171]
44. Lester WM, Damji AA, Gedeon I, Tanaka M. Interstitial cells from the atrial and ventricular sides of the bovine mitral valve respond differently to denuding endocardial injury. In Vitro Cell Dev Biol 1993;29A:41–50. [PubMed: 8095255]
45. Ng CM, Cheng A, Myers LA, Martinez-Murillo F, Jie C, Bedja D, Gabrielson KL, Hausladen JM, Mecham RP, Judge DP, Dietz HC. TGF-beta-dependent pathogenesis of mitral valve prolapse in a mouse model of Marfan syndrome. J Clin Invest 2004;114:1586–1592. [PubMed: 15546004]
46. Ku CH, Johnson PH, Batten P, Sarathchandra P, Chambers RC, Taylor PM, Yacoub MH, Chester AH. Collagen synthesis by mesenchymal stem cells and aortic valve interstitial cells in response to mechanical stretch. Cardiovasc Res 2006;71:548–556. [PubMed: 16740254]
47. Quick DW, Kunzelman KS, Kneebone JM, Cochran RP. Collagen synthesis is upregulated in mitral valves subjected to altered stress. Asaio J 1997;43:181–186. [PubMed: 9152488]
48. Dewald O, Ren G, Duerr GD, Zoerlein M, Klemm C, Gersch C, Tincey S, Michael LH, Entman ML, Frangogiannis NG. Of mice and dogs: species-specific differences in the inflammatory response following myocardial infarction. Am J Pathol 2004;164:665–677. [PubMed: 14742270]
49. Kunzelman KS, Quick DW, Cochran RP. Altered collagen concentration in mitral valve leaflets: biochemical and finite element analysis. Ann Thorac Surg 1998;66:S198–205. [PubMed: 9930448]
50. Paruchuri S, Yang JH, Aikawa E, Melero-Martin JM, Khan ZA, Loukogeorgakis S, Schoen FJ, Bischoff J. Human pulmonary valve progenitor cells exhibit endothelial/mesenchymal plasticity in response to vascular endothelial growth factor-A and transforming growth factor-beta2. Circ Res 2006;99:861–869. [PubMed: 16973908]

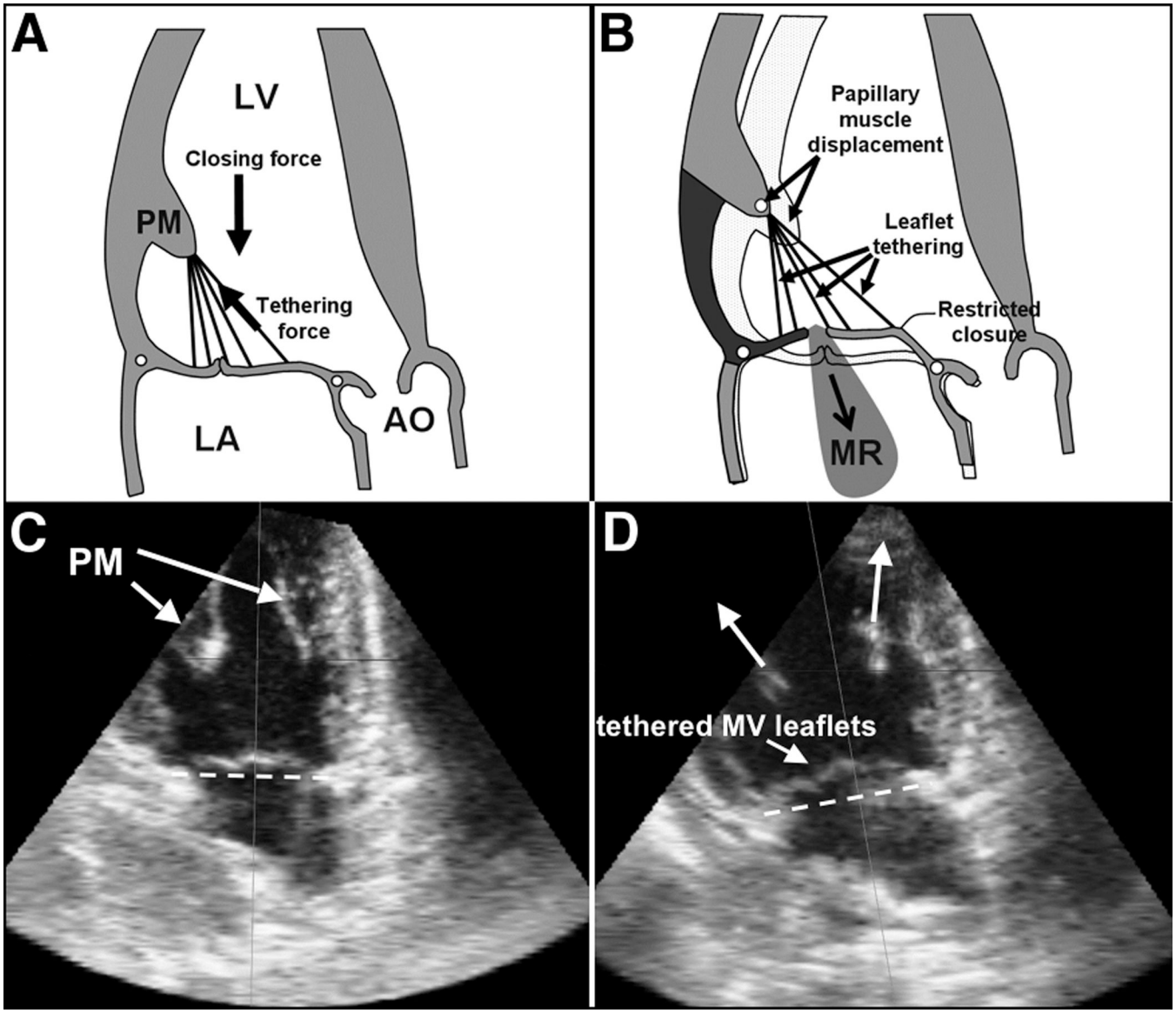

Figure 1.

Normal MV closure (A,C); effect of apical and posterior shift of PMs restraining the MV, causing MV leaflet tethering (D) and, if severe enough, MR (B). Lower panel (C & D): Echocardiography of the LV (apical two-chamber view) in the same sheep prior to (C) and after pulling the PMs apically resulting in MV leaflet tethering (D). The dashed line indicates the mitral annular level. (Ao: Aorta, LA: left atrium; LV: left ventricle, MR: mitral regurgitation; MV: mitral valve; PM: papillary muscle) (Figures A & B adapted from Levine et al [14]).

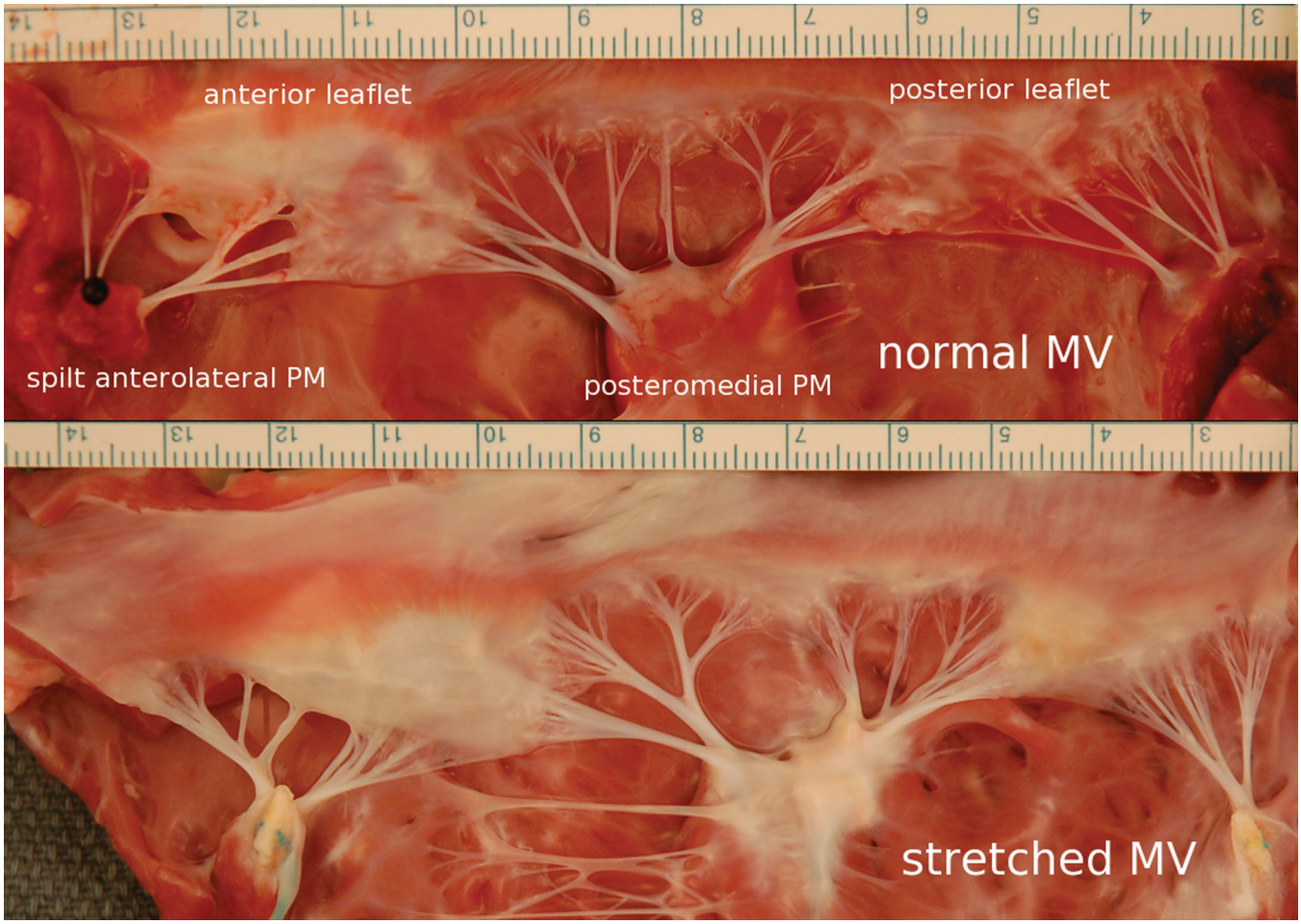

Figure 2.
Normal MV (upper panel) versus stretched MV leaflets (lower panel), which are less opaque consistent with increased thickness. (PM: papillary muscle; units in cm).

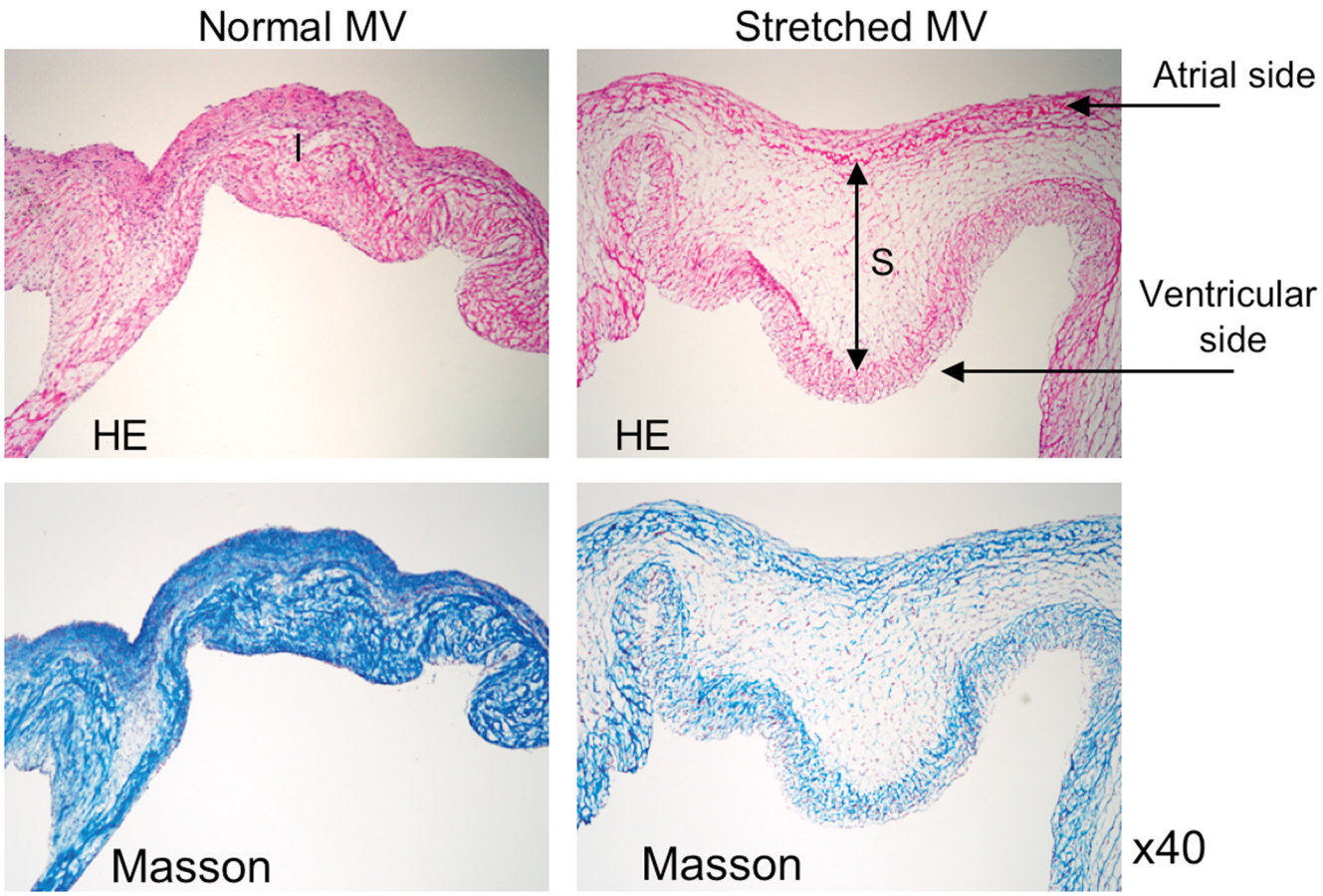

Figure 3.
Hematoxylin & eosin (HE) and Masson staining in the normal (left) and stretched MV (right) demonstrating increased spongiosa layer thickness. (Blue=collagen)

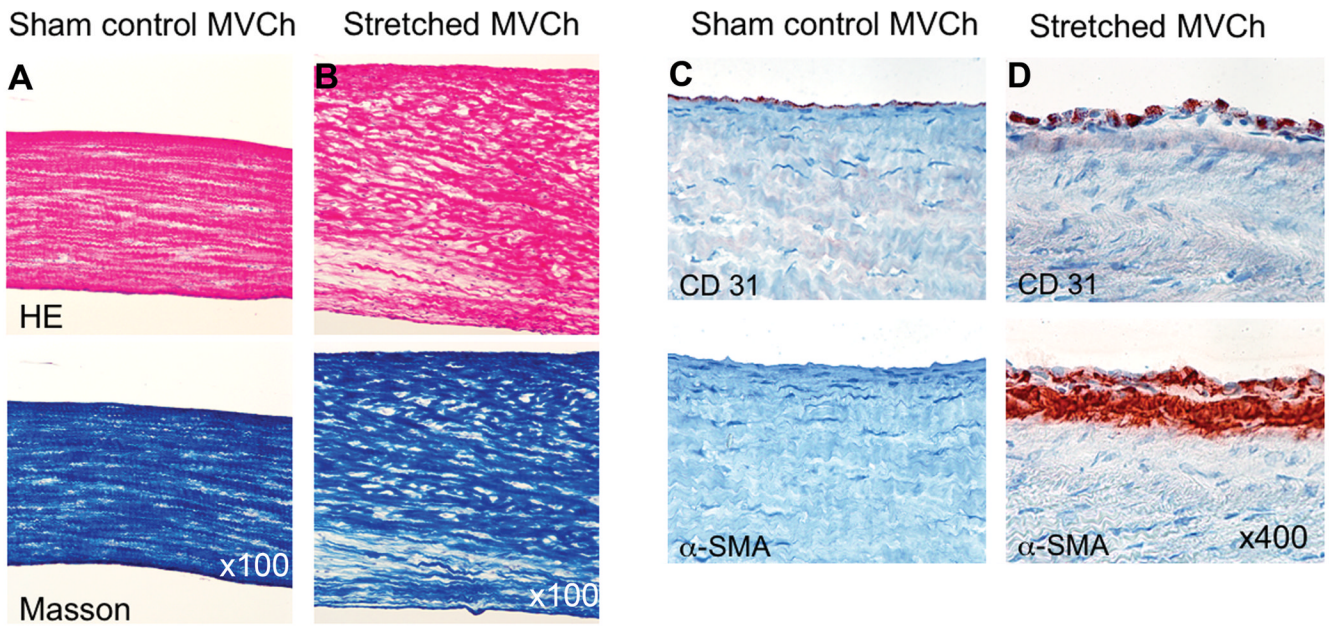

Figure 4.

A&B: Stretched chordae are significantly thicker and have decreased collagen alignment and density compared to unstretched chordae. C&D: Stretched chordae show endothelial-cell α-SMA-positive staining and subendothelial accumulation of α-SMA-positive myofibroblasts.

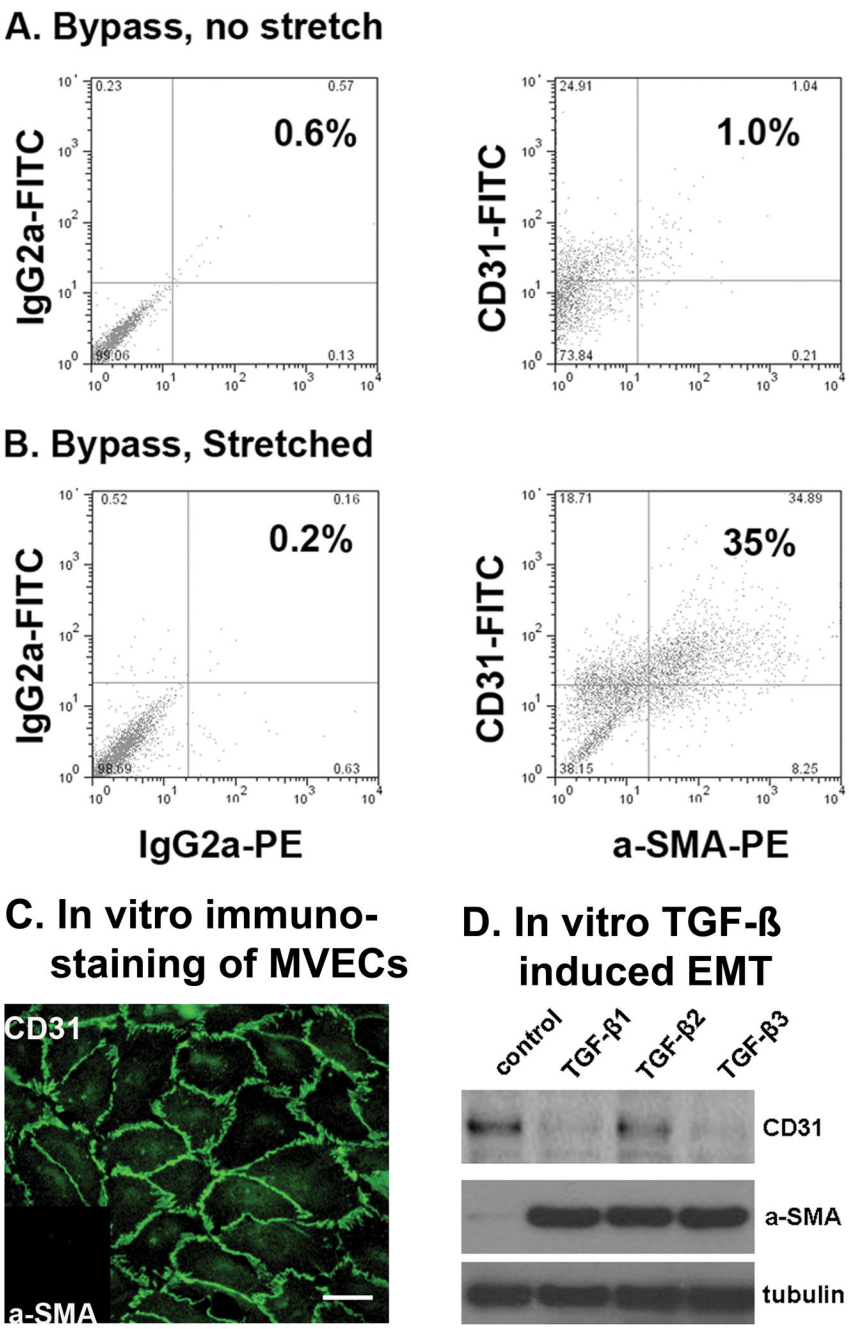

Figure 5.

Increased endothelial cells (CD31+) also expressing α-SMA in stretched versus unstretched MVs (A,B). Left: representative sample of cells double-labeled with isotype-matched control antibodies. Right: cells double-labeled with anti-sheep CD31 conjugated to FITC and anti-α-SMA conjugated to phycoerthrin (PE). Compensation was performed with singly labeled cells (not shown).

C&D: MV ECs undergo TGF-β-induced EMT in vitro. C: Immunostained MV ECs showing CD31 localized at cell-cell borders and α-SMA was undetectable (inset), confirming endothelial phenotype. Scale bar, 50μm. D: Western blots of lysates from MV ECs treated with

1ng/ml TGF-β1, TGF-β2, or TGF-β3 for 5 days. All three TGF-β isoforms induced expression of α-SMA.

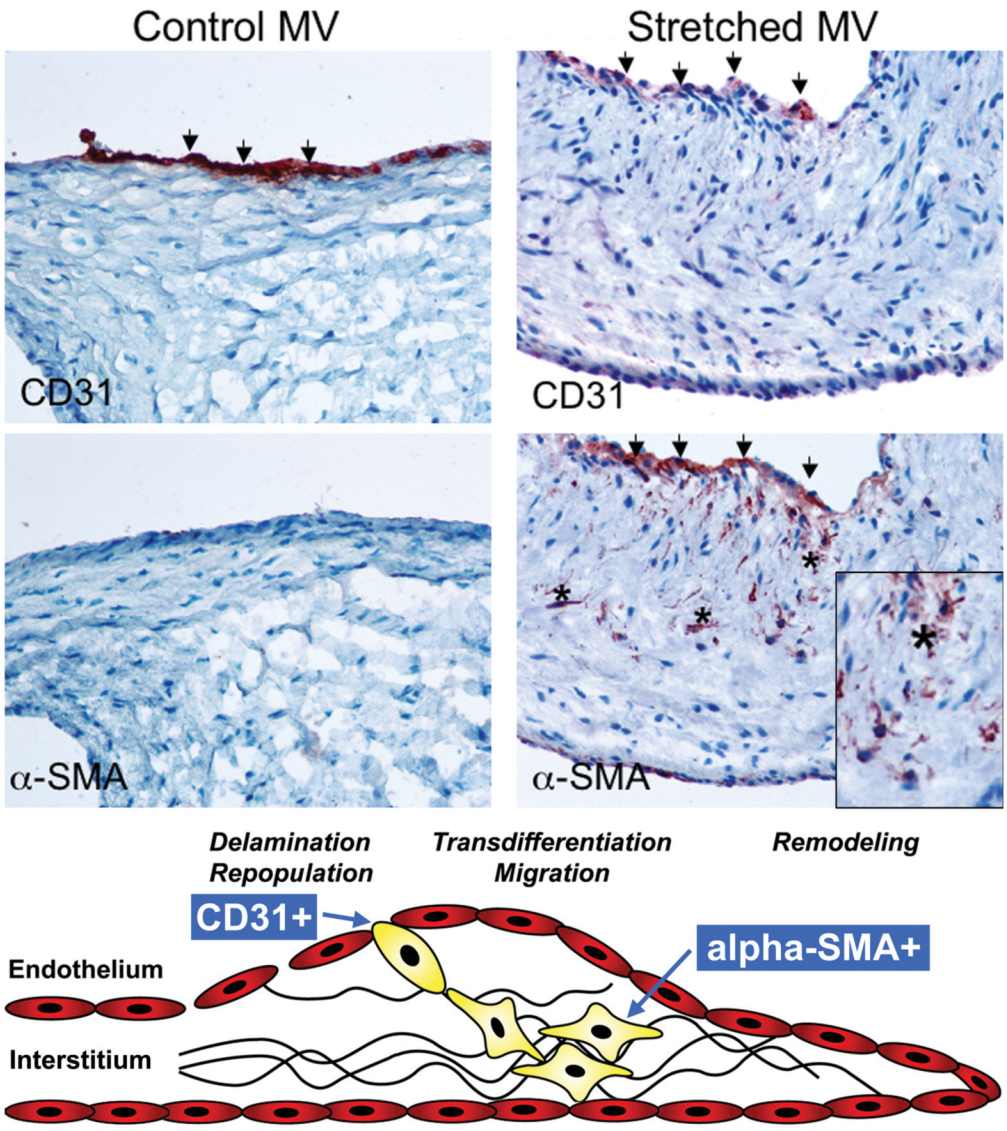

Figure 6.

Left: Unstretched MV showing negative α-SMA staining along the CD31+ endothelium. Right: α-SMA+ staining in the atrial endothelium (also CD31+) of a stretched MV, with nests of α-SMA+ cells appearing to penetrate the interstitium (asterisks, below). Lower panel: Schematic of active mitral valve adaptation by EMT (adapted from Armstrong et al [36]). (α-SMA: α-smooth muscle actin)

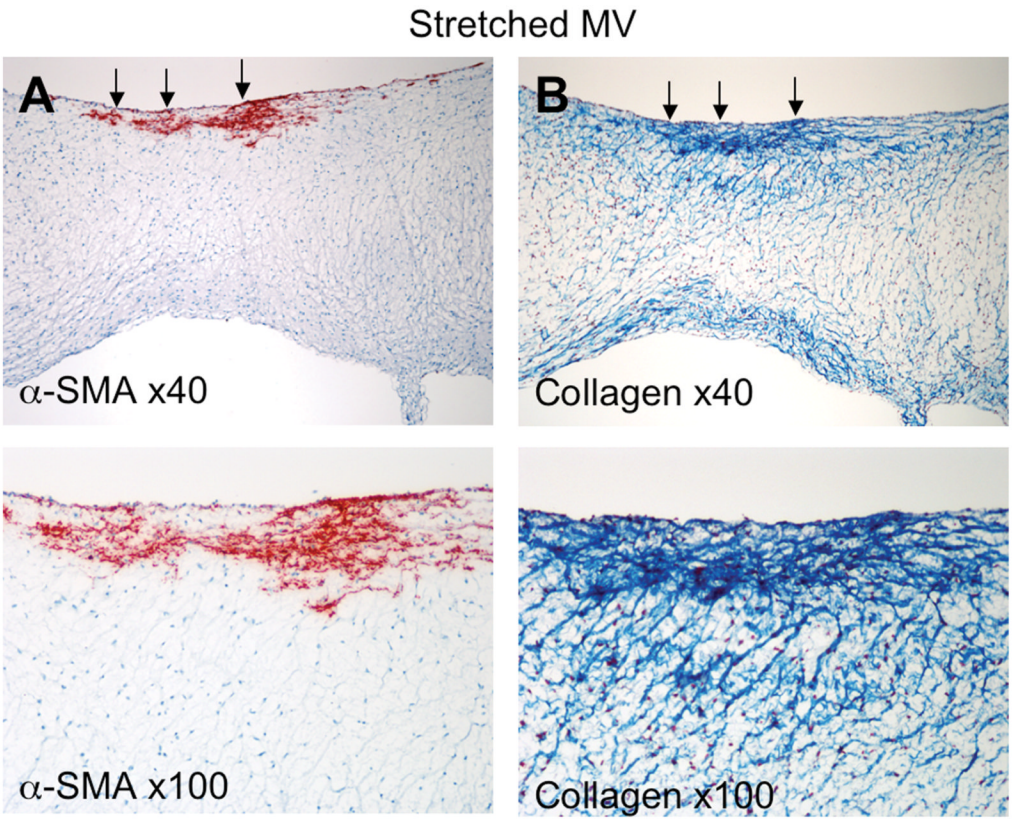

Figure 7.
Stretched MV: α-SMA-positive cells penetrating from the atrial surface into the valve interstitium (A) with increased collagen deposition in the same region (B).

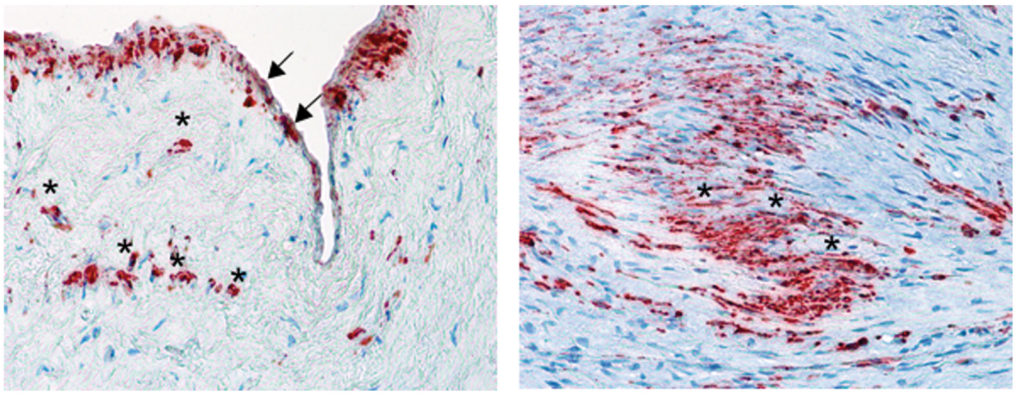

Figure 8.
α-SMA-positive cells in a patient with ischemic MR in the atrial endothelium (left, arrows) and throughout the interstitium (asterisks).

Table 1

Echocardiographic Baseline and Sacrifice Parameters of Sheep with Stretched Leaflets

	Baseline	Sacrifice	p
LVEDV (ml)	58±13	62±13	0.32
LVESV (ml)	25±9	31±8	0.14
LVEF %	57±6	54±6	0.07
MV leaflet area (cm^2)	14.3±1.9	16.7±1.9	0.006
Leaflet length A2 (mm)	17.4±1.3	19.4±1.5	0.02
Leaflet length P2 (mm)	14.6±1.9	15.9±1.7	0.02
Annular area (diastole, cm^2)	8.35±1.57	9.64±1.38	0.03
Annulus AP diameter (cm)	2.7±0.4	3.2±0.2	0.06
Annulus CC diameter (cm)	3.8±0.4	3.8±0.5	1
Tenting volume (cm^3)	1.67±0.59	3.26±0.91	0.02
Vena contracta (cm)	0.07±0.12	0.12±0.19	0.6

Student's paired t-test, two-sided

A2: anterior MV leaflet, middle scallop; AP: anteroposterior; CC: commissure-to-commissure; LVEDV: left ventricular enddiastolic volume; LVESV: left ventricular endsystolic volume; LVEF: left ventricular ejection fraction; MV: mitral valve; P2: posterior MV leaflet, middle scallop;

Table 2

Mitral Valve Leaflet and Chordal Characteristics in Sham Sheep versus Sheep with Stretched Leaflets

	Sham	Stretched	p
MV leaflet thickness base (mm)	0.72±0.2	1.18±0.35	0.02
MV leaflet thickness mid (mm)	0.42±0.14	1.18±0.43	<0.0001
MV leaflet thickness tip (mm)	0.18±0.04	0.32±0.13	0.002
Anterior strut chord length (mm)	20.3±2.6	24.3±2.5	0.032
Anterior strut chord diameter (mm)	1.0±0.1	1.2±0.1	0.026
Posterior strut chord length (mm)	16.9±1.3	18.9±1.1	0.029
Posterior strut chord diameter (mm)	0.8±0.02	1.1±0.1	0.017
Averaged chordal diameter (mm)	0.59±0.21	0.96±0.07	<0.0001

Student's t-test, two-sided

MV: mitral valve;